Available online at www.sciencedirect.com
ScienceDirect
Proceedings of the Combustion Institute 31 (2007) 1641–1648
Proceedings of the Combustion Institute
www.elsevier.com/locate/proci

# Direct numerical simulation of turbulence–radiation interactions in homogeneous nonpremixed combustion systems

K.V. Deshmukh *, D.C. Haworth, M.F. Modest

*Department of Mechanical and Nuclear Engineering, The Pennsylvania State University, University Park, PA, USA*



**Abstract**

An important issue in chemically reacting turbulent flows is the interaction between turbulence and radiation (turbulence–radiation interactions—TRI). TRI arises from highly nonlinear coupling between fluctuations in temperature and species composition with the fluctuations of radiative intensity. Here direct numerical simulation (DNS) has been employed to investigate TRI in a statistically homogeneous nonpremixed system. A photon Monte Carlo method has been used to solve the radiative transfer equation (RTE). Radiation properties correspond to a nonscattering fictitious gray gas with a Planck-mean absorption coefficient that mimics that of typical hydrocarbon-air combustion products. Individual contributions of emission and absorption TRI have been isolated and quantified. The temperature self-correlation, the absorption coefficient-Planck function correlation, and the absorption coefficient-intensity correlation have been examined for intermediate-to-large values of the optical thickness, and contributions from all three correlations have been found to be significant. Emission TRI has also been estimated analytically using a $\beta$ PDF model. The $\beta$ PDF results are in good agreement with DNS results. This suggests that relatively simple models for emission TRI in nonpremixed systems might be developed based on a modeled equation for mixture fraction variance.


*Keywords:* Turbulence–radiation interactions; Direct numerical simulation; Photon Monte Carlo method

## 1. Introduction

Most practical combustion devices involve turbulent fluid flow, and the high temperatures prevalent in most combustion processes result in substantial heat transfer by radiation. Accurate descriptions of turbulence and combustion are already mathematically complex and computationally expensive. That often has resulted in the neglect of radiation or treatment of radiation using simple models in turbulent combustion applications, to avoid the additional complexity of solving the radiative transfer equation (RTE) [1].

The importance of interactions between turbulence and thermal radiation (turbulence–radiation interactions—TRI) has long been recognized [2–8]. TRI is known to result in increased radiative emission, reduced temperatures, and consequently significant changes in key pollutant species (particularly $NO_x$ and soot) in chemically reacting turbulent flows. TRI arises from the highly nonlinear

* Corresponding author. Fax: +1 814 865 3389.
*E-mail address:* kvd107@psu.edu (K.V. Deshmukh).

1540-7489/$ - see front matter © 2006 The Combustion Institute. Published by Elsevier Inc. All rights reserved.
doi:10.1016/j.proci.2006.07.139

coupling between temperature, composition and radiative intensity fluctuations. Li and Modest [8] showed an approximately 30% increase in radiative flux with TRI compared to thermal radiation without TRI in their modeling study of nonpremixed turbulent jet flames. Coelho [9] reported a nearly 50% increase in radiative heat loss due to TRI for a nonpremixed methane/air turbulent jet flame, while Tessé et al. [10] reported 30% increase in radiative heat loss with consideration of TRI for a sooty nonpremixed ethylene/air turbulent jet flame. Wu et al. [11] studied TRI for an idealized turbulent premixed flame using direct numerical simulation (DNS) coupled with a photon Monte Carlo method for the solution of the RTE; they found that emission and absorption both are enhanced when TRI are considered, and that the effects remained important even at relatively low optical thicknesses.

Here DNS coupled with a radiation photon Monte Carlo method [11,12] is used to isolate and quantify TRI effects in an idealized nonpremixed system. The aims are to provide new fundamental physical insight into TRI in chemically reacting turbulent flows and to provide guidance for model development. The nature of turbulence–radiation interactions is discussed in Section 2. The model problem is outlined in Section 3, and results and discussion are provided in Section 4. Conclusions and next steps are summarized in the final section.

## 2. Turbulence–radiation interactions

The RTE is an integro-differential equation for the radiative intensity [1]. A general form of the RTE for the spectral radiative intensity $I_\eta$ is:

$$\frac{\mathrm{d}I_\eta}{\mathrm{d}s} = \hat{s}\cdot\nabla I_\eta = \kappa_\eta I_{b\eta} - \beta_\eta I_\eta + \frac{\sigma_{s\eta}}{4\pi} \times \int_{4\pi} I_\eta(\hat{s}_i)\Phi_\eta(\hat{s}_i,\hat{s})\,\mathrm{d}\Omega_i. \quad (1)$$

Here $\hat{s}$ and $\hat{s}_i$ denote unit direction vectors, $\eta$ denotes wavenumber, $\Omega$ is solid angle, $\kappa_\eta$ is the spectral absorption coefficient, $I_{b\eta}$ is the Planck function (a known function of local temperature and wavenumber), $\sigma_{s\eta}$ is the spectral scattering coefficient, and $\beta_\eta = \kappa_\eta + \sigma_{s\eta}$ is the spectral extinction coefficient. The function $\Phi_\eta(\hat{s}_i,\hat{s})$ is the scattering phase function; it describes the probability that a ray from incident direction $\hat{s}_i$ is scattered into direction $\hat{s}$. The local value of $I_\eta$ depends on nonlocal quantities, on direction $\hat{s}$, and on wavenumber. The RTE is a radiation balance for an infinitesimal pencil of rays. In combustion applications, one needs the net radiative energy transfer (radiative energy deposited or withdrawn per unit volume) for each volume element in the medium. This is obtained by integrating the RTE over all solid angles and all wavenumbers. The net radiative energy per unit volume (the radiation source term in the energy equation) is then:

$$\nabla\cdot\vec{q}_{\mathrm{rad}} = \int_0^\infty \kappa_\eta\left(4\pi I_{b\eta} - \int_{4\pi} I_\eta\,\mathrm{d}\Omega\right)\mathrm{d}\eta = 4\kappa_{\mathrm{P}}\sigma T^4 - \int_0^\infty\int_{4\pi}\kappa_\eta I_\eta\,\mathrm{d}\Omega\,\mathrm{d}\eta. \quad (2)$$

Here $\vec{q}_{\mathrm{rad}}$ is the radiative heat flux, $\sigma$ is the Stefan–Boltzmann constant, and $\kappa_{\mathrm{P}}$ is the Planck-mean absorption coefficient:

$$\kappa_{\mathrm{P}} \equiv \frac{\int_0^\infty \kappa_\eta I_{b\eta}\,\mathrm{d}\eta}{\int_0^\infty I_{b\eta}\,\mathrm{d}\eta} = \frac{\pi}{\sigma T^4}\int_0^\infty \kappa_\eta I_{b\eta}\,\mathrm{d}\eta. \quad (3)$$

For the case of a gray medium ($\kappa_\eta = \kappa$), Eq. (2) reduces to

$$\nabla\cdot\vec{q}_{\mathrm{rad}} = 4\kappa_{\mathrm{P}}\sigma T^4 - \kappa_{\mathrm{P}} G, \quad (4)$$

where $G \equiv \int_{4\pi} I\,\mathrm{d}\Omega$ is the direction-integrated incident radiation. The first term on the right-hand side of Eq. (2) or Eq. (4) corresponds to emission and the second to absorption. TRI is brought into evidence by taking the mean of Eq. (4):

$$\langle\nabla\cdot\vec{q}_{\mathrm{rad}}\rangle = 4\sigma\langle\kappa_{\mathrm{P}}T^4\rangle - \langle\kappa_{\mathrm{P}}G\rangle, \quad (5)$$

where angled brackets denote mean quantities.

In the emission term, TRI appears as a correlation between the Planck-mean absorption coefficient and the fourth power of temperature (the simplified Planck function, $I_b$): $\langle\kappa_{\mathrm{P}}T^4\rangle = \langle\kappa_{\mathrm{P}}\rangle\langle T^4\rangle + \langle\kappa'_{\mathrm{P}}\cdot(T^4)'\rangle$, where a prime denotes a fluctuation about the local mean. Emission TRI usually is decomposed to consider separately the temperature self-correlation ($\langle T^4\rangle \neq \langle T\rangle^4$) and the absorption coefficient—Planck function correlation. In the absorption term, TRI appears as a correlation between the absorption coefficient and the incident radiation, $\langle\kappa_{\mathrm{P}}G\rangle = \langle\kappa_{\mathrm{P}}\rangle\langle G\rangle + \langle\kappa'_{\mathrm{P}}G'\rangle$.

In the present study, we explore TRI in a statistically homogeneous nonstationary turbulent nonpremixed system using DNS. The principal quantities examined are the normalized means $\mathcal{R}_{T^4}$, $\mathcal{R}_{\kappa I_b}$, and $\mathcal{R}_{\kappa G}$

$$\mathcal{R}_{T^4} \equiv \frac{\langle T^4\rangle}{\langle T\rangle^4}, \quad \mathcal{R}_{\kappa I_b} \equiv \frac{\langle\kappa'_{\mathrm{P}}I'_b\rangle}{\langle\kappa_{\mathrm{P}}\rangle\langle I_b\rangle}, \quad \mathcal{R}_{\kappa G} \equiv \frac{\langle\kappa'_{\mathrm{P}}G'\rangle}{\langle\kappa_{\mathrm{P}}\rangle\langle G\rangle}. \quad (6)$$

In the absence of TRI, $\mathcal{R}_{T^4}$ would be equal to one, and $\mathcal{R}_{\kappa I_b}$ and $\mathcal{R}_{\kappa G}$ would each be equal to zero. The departures of each quantity from these values allow different contributions to TRI to be isolated and quantified.

A dimensionless optical thickness $\kappa L$ is introduced, where $L$ is an appropriate length scale. Kabashnikov and co-workers [13–15] suggested

that if the mean free path for radiation is much larger than the turbulence eddy length scale, then the fluctuations in $\kappa$ (a quantity dependent on local properties) should be uncorrelated with those in $G$ (a nonlocal quantity), so that $\langle\kappa G\rangle \approx \langle\kappa\rangle\langle G\rangle$: this is the "optically thin eddy" approximation ($\kappa L \ll 1$). At the other extreme ($\kappa L \gg 1$), the optical thickness may be large compared to *all* hydrodynamic and chemical scales. In that case, fluctuations in intensity are generated locally and would be expected to be correlated strongly with those of the absorption coefficient: a diffusion approximation is appropriate in that case [1]. Between these extremes are cases where the smallest scales (Kolmogorov microscales and/or flame thickness) are optically thin while the largest (integral scales) are optically thick. Modeling of such intermediate cases is an outstanding challenge in TRI, and is the primary motivation for this study.

## 3. Physical and numerical models

### 3.1. Computational configuration

A statistically homogeneous isotropic nonstationary (decaying) turbulent nonpremixed system is considered (Fig. 1). The configuration is a cube of sides $2\pi$ with 64 grid nodes in each direction; the system is periodic in the $x$-, $y$- and $z$-directions to represent an unbounded domain.

### 3.2. Physical models

The continuity, linear momentum, chemical species, and energy equations have the same form as in [16]. Nondimensional forms of the governing equations are solved. Chemistry is taken to be infinitely fast (infinite Damköhler number $Da$) and the participating medium to be nonscattering and gray. Moreover, the chemistry and the radiation are passive with respect to the fluid dynamics, i.e., the chemical and radiative source terms do not feed back into the energy equation. This precludes extracting information on the effects of radiation on the turbulent flow field, but is appropriate for this initial investigation of TRI quantities discussed in Section 2 for nonpremixed turbulent systems. A one-step irreversible reaction is considered wherein fuel (F) and oxidizer (O) react to form products (P):

$$\mathrm{F} + \mathrm{O} \rightarrow \mathrm{P}. \tag{7}$$

A conserved-scalar mixture fraction $\xi$ is introduced to characterize mixing of the species: $\xi = 1.0$ for pure fuel, $\xi = 0.0$ for pure oxidizer, and $\xi = \xi_{st} = 0.5$ for stoichiometric proportions (pure products). The choice of stoichiometric value enables equal detailed study on either side of stoichiometry, as against a realistic value of 0.05. Standard molecular transport models (Newtonian viscosity, Fourier conduction, and Fickian species diffusion) are employed where the molecular transport coefficients (viscosity $\mu$, thermal conductivity $\lambda$, and species diffusion coefficient $\mathcal{D}$) are set such that the Prandtl number $Pr = 0.75$ and Lewis number $Le = 1.0$ are constant. The viscosity of the fluid is constant. Soret and Dufour effects are not included. The working fluid is an ideal gas with constant ratio of specific heats, $\gamma = 1.4$.

An initial turbulence spectrum is prescribed using methods outlined in [16,17] and the initial mixture fraction field is prescribed following the approach of Eswaran and Pope [18]. The initial mixture fraction field conforms approximately to double-delta-function probability density function (PDF), corresponding to pure fuel or pure oxidizer at every location. An exact double-delta-function would result in steep scalar gradients that

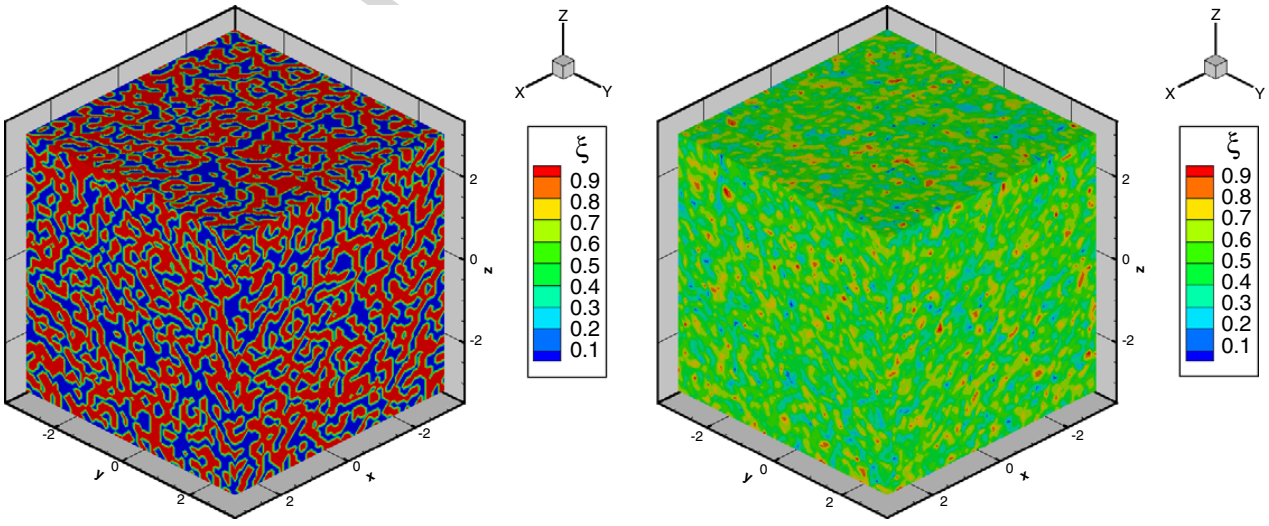


Fig. 1. The three-dimensional mixture fraction field at time $t/\tau = 0.0$ (left) and time $t/\tau = 0.4$ (right).

cannot be resolved numerically. Hence, the double-delta-function is smoothed spatially just enough so that it can be supported on the mesh. The PDF of the scalar tends to a Gaussian as it evolves in time as shown in Fig. 2 (left).

Figure 1 shows the initial three-dimensional mixture fraction field on the left and the evolved mixture fraction at time $t/\tau = 0.4$ on the right. Here $\tau$ is the turbulence integral time scale for the initial turbulent field. The initial pockets of fuel and oxidizer react to form products, so that the box contains essentially pure products by time $t/\tau = 1.4$.

Radiation properties correspond to a fictitious nonscattering gray gas with Planck-mean absorption coefficient

$$\kappa_p = C_\kappa (Y_P + \epsilon_Y)\left[c_0 + c_1\left(\frac{A}{T}\right) + c_2\left(\frac{A}{T}\right)^2 + c_3\left(\frac{A}{T}\right)^3 + c_4\left(\frac{A}{T}\right)^4 + c_5\left(\frac{A}{T}\right)^5\right]. \quad (8)$$

Coefficients $A$ and $c_0$–$c_5$ have been taken from a radiation model suggested for water vapor [19]. Here $\epsilon_Y$ is an arbitrary, small, positive threshold to ensure that $\kappa_P$ is nonzero everywhere, and $C_\kappa$ is a coefficient that allows the optical thickness to be varied systematically and independently of other parameters. For fixed values of $C_\kappa$ and $Y_P$, $\kappa_P$ varies by more than a factor of 10 over the temperature range of interest. In Eq. (8), $Y_P$ is the product mass fraction, which is a linear function of mixture fraction $\xi$ (Fig. 3)

$$Y_P = \begin{cases} \xi/\xi_{st}, & \text{if } \xi \leqslant \xi_{st}, \\ (1-\xi)/(1-\xi_{st}), & \text{if } \xi > \xi_{st}. \end{cases} \quad (9)$$

The temperature is re-scaled to the computational temperature range and, consistent with the simplified thermochemistry, is taken to be a linear function of $Y_P$:

$$T = T_{min} + (T_{max} - T_{min}) \times Y_P, \quad (10)$$

where the nondimensional $T_{min}$ and $T_{max}$ are fixed to 2.5 and 10.0, corresponding to 300 and 1200 K, respectively. With these simplifications, $Y_F$, $Y_O$, $Y_P$, $T$, and $\kappa_P$ are unique functions of $\xi$, as shown in Fig. 3. These forms are consistent with a fast-chemistry limit ($Da \to \infty$). An optical thickness $\kappa_{P,2} l_{11}$ based on burned-gas ($Y_P = 1.0$) properties and the initial turbulence integral length scale $l_{11}$ characterizes thermal radiation.

Simulation parameters are summarized in Table 1. The correlations of Eq. (6) are studied for two values of the optical thickness: (a) an optically thick case, $\kappa_{P,2} l_{11} = 10$; and (b) optically intermediate case, $\kappa_{P,2} l_{11} = 1$. The quantity $l_\xi$ is the scalar integral length scale of the initial mixture fraction field. The turbulent Reynolds number is defined as $Re = u'_{rms} l_{11}/\nu$, where $u'_{rms}$ is the RMS turbulence velocity for the initial turbulent field and $\nu$ is kinematic viscosity.

### 3.3. Numerical methods

Temporal integration is performed with a Runge-Kutta method of order three; for spatial discretization, a compact scheme of order six is used in the interior of the computational domain with non-centered schemes near boundaries [20]. Details of the equations, normalizations, and numerical methods (in the absence of thermal radiation) can be found in [17].

The RTE is solved using a photon Monte Carlo method, wherein the trajectories of a large number of representative photon bundles generated using statistical sampling techniques are followed [1,11,12]. The photon Monte Carlo

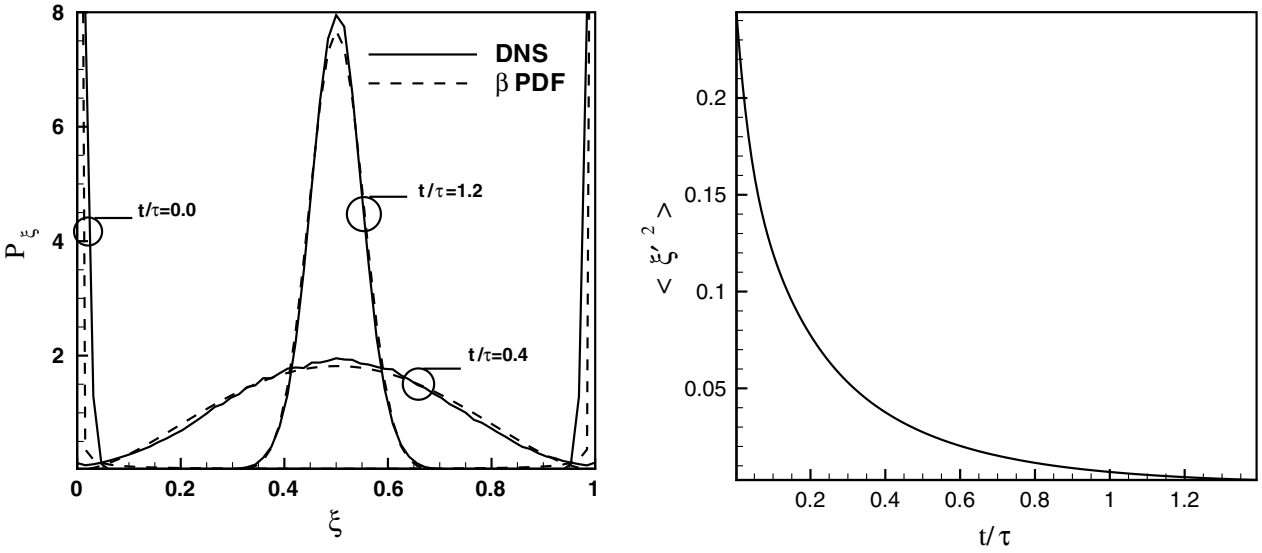


Fig. 2. The evolution of the PDF of mixture fraction (left) and the decay of variance of mixture fraction (right) as function of the nondimensional time.

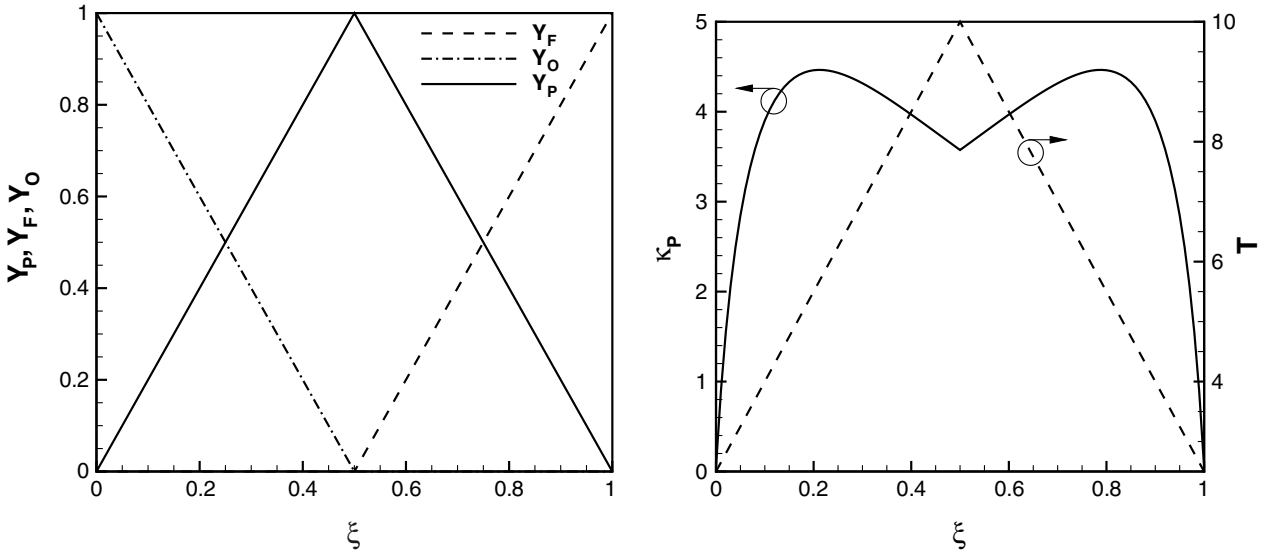


Fig. 3. Three species mass fractions (left), and temperature $T$ and absorption coefficient $\kappa_P$ (right) as functions of mixture fraction $\xi$.

Table 1
Simulation parameters

| Case | Grid | $\kappa_{P,2} l_{11}$ | $l_{11}$ | $l_\xi$ | $Re$ |
|---|---|---|---|---|---|
| Case 1 | $64^3$ | 1.0 | 0.52 | 0.112 | 105 |
| Case 2 | $64^3$ | 10.0 | 0.52 | 0.112 | 105 |

In all cases: $Da \sim \infty$, $Pr = 0.75$, $Le = 1.0$, and $\gamma = 1.4$.

method for a participating medium consists of two parts: an emission stage and a tracing/absorption stage. For the periodic boundaries that are considered here, a photon bundle that exits through one face simply reenters the corresponding location on the opposite face with its direction and properties unchanged. Each emitted photon bundle is traced until its energy is depleted to zero. Details for the photon Monte Carlo method, including issues of numerical accuracy and computational efficiency, can be found in [12]. Here third-order accurate schemes in space have been employed for the photon Monte Carlo method.

Because chemistry and radiation are uncoupled from the fluid dynamics, the simulations correspond to investigations of TRI effects for an essentially frozen turbulence field at every timestep. Moreover, because of the form that has been adopted for $\kappa_P(Y_P, T)$ (Eq. (8)), the emission TRI, which depends only on the local properties, is independent of the optical thickness, as the latter is varied by changing $C_\kappa$ in Eq. (8). Absorption TRI, however, depends on nonlocal quantities and will vary depending on the optical thickness.

## 4. Results and discussion

The numerical simulations were carried out using a $64^3$ computational grid, and tracing $10^7$ photon bundles per time step. A parallel implementation using MPI was used to speed up the photon Monte Carlo calculations. The computational time required for the optically thick case was 26 h and for the optically intermediate case was 300 h on 4 Dual 3.2 GHz Intel Xeon Processors with High Speed Myrinet Network, of which 96% was taken up by the photon Monte Carlo Method. Mean quantities are estimated by averaging over all grid points for this statistically homogeneous configuration. Figure 2 (right) shows the decay in the variance of mixture fraction as function of nondimensional time; the mean of mixture fraction is constant and is equal to 0.5 throughout the run. The decay of the mixture fraction variance implies that the fluctuations in all the quantities that are functions of the mixture fraction (Fig. 3) are also reducing. For the system as a whole, the initial fuel and oxidizer are consumed and the domain is increasingly filled with hot products as the simulation proceeds. Simulations are stopped at $t/\tau = 1.4$ as the domain is filled with more than 90% products by that time, and fluctuations have decayed to the point where no additional useful information can be extracted.

### 4.1. Emission TRI

The temperature self-correlation factor $\mathcal{R}_{T^4}$ is plotted as function of the nondimensional time in Fig. 4. The evolution of the temperature and species fields, and therefore the evolution of $\kappa_P(Y_P, T)$, are determined by the evolution of the mixture fraction field in this configuration. The temperature self-correlation factor initially is close to unity, corresponding to the initial approximate double-delta-function PDF (Fig. 2). It increases rapidly to a peak value of about 3 at $t/\tau = 0.08$,

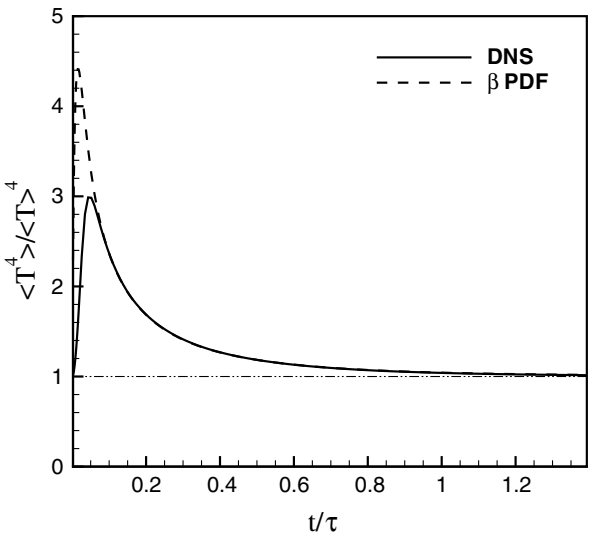


Fig. 4. Evolution of temperature self-correlation factor $\mathcal{R}_{T^4}$ with nondimensional time.

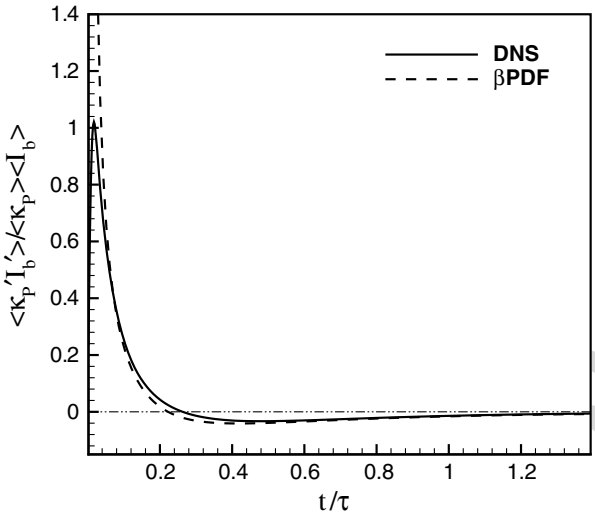


Fig. 5. Evolution of absorption coefficient—Planck function correlation factor $\mathcal{R}_{\kappa I_b}$ with nondimensional time.

then decays slowly back to unity as the fluctuations in $\xi$, and hence $T$, decay towards zero. The horizontal dash-dot-dot reference line in Fig. 4 corresponds $\mathcal{R}_{T^4} = 0$ (absence of temperature self-correlation TRI).

The evolution of the emission TRI factor $\mathcal{R}_{\kappa I_b}$ is plotted in Fig. 5. The trend for $\mathcal{R}_{\kappa I_b}$ is similar to that for temperature self-correlation, and $\mathcal{R}_{\kappa I_b}$ is the same for both optical thicknesses as discussed in Section 3.3. Initially, the PDF of the mixture fraction field is close to a double-delta-function; while the fluctuations in mixture fraction are initially large (Fig. 2), most of the domain corresponds to either pure fuel or to pure oxidizer so that $\langle \kappa_P' I_b' \rangle$ is close to zero. As time increases, both $T$ and $\kappa_P$ increase with fluctuations in $\xi$ away from zero or one (Fig. 3), leading to a high positive value of $\langle \kappa_P' I_b' \rangle$. As the system continues to evolve, $\mathcal{R}_{\kappa I_b}$ decays and eventually becomes negative, then approaches zero through negative values as $t/\tau$ increases. This behavior can be understood from Fig. 3. As $\xi$ approaches $\xi_{st} = 0.5$ from either the fuel side or the oxidizer side, the decrease in $\kappa_P$ with increasing $T$ dominates the increase in $\kappa_P$ with increasing $Y_P$ (Eq. (8)), such that $\langle \kappa_P' I_b' \rangle < 0$. Here $\mathcal{R}_{\kappa I_b} > 0$ corresponds to enhanced radiative emission via TRI, and $\mathcal{R}_{\kappa I_b} < 0$ to reduced radiative emission via TRI. The horizontal dash-dot-dot reference line in Fig. 5 corresponds $\mathcal{R}_{\kappa I_b} = 0$ (absence of emission TRI).

Emission TRI can be approximated analytically for this configuration. Given the knowledge of the mean $\langle \xi \rangle$ and the variance $\langle \xi'^2 \rangle$ of the mixture fraction $\xi$, the PDF of mixture fraction $P(\xi)$ is modeled as a $\beta$-distribution [21] as:

$$P(\xi) = \frac{\xi^{a-1}(1-\xi)^{b-1}\Gamma(a+b)}{\Gamma(a)\Gamma(b)},$$
$$a = \langle \xi \rangle \left( \frac{\langle \xi \rangle (1 - \langle \xi \rangle)}{\langle \xi'^2 \rangle} - 1 \right), \qquad (11)$$
$$b = (a/\langle \xi \rangle) - a,$$

where the gamma function $\Gamma(z)$ is defined as $\Gamma(z) = \int_0^\infty t^{z-1} e^{-t}\, dt$. With the PDF modeled using Eq. (11), it is possible to compute emission TRI correlations since $Y_P$, $T$, and $\kappa_P$ are unique functions of $\xi$ (Fig. 3) and since

$$\langle f(\xi) \rangle = \int_0^1 f(\xi) P(\xi)\, d\xi, \qquad (12)$$

for any $f = f(\xi)$. This is how the curves labeled '$\beta$ PDF' in Figs. 2, 4, and 5 were obtained. The actual values agree well with those obtained using the $\beta$ PDF except at early times. This is because the PDF of the mixture fraction only approximates a $\beta$ function at early times, as a result of the smoothened initial mixture fraction field (not a pure double-delta-function).

Emission TRI contributions are seen to be significant even for this idealized uncoupled system. In the case of finite-rate chemistry and chemical and radiative source feedback into the energy equation, the situation would be more complex. However, the success of the $\beta$ PDF model here suggests that relatively simple models for emission TRI in nonpremixed systems might be developed based on solving modeled transport equations for the mean and the variance of a mixture fraction. The $\beta$ PDF model, a single point PDF, cannot predict the absorption TRI, a effect influenced by nonlocal properties.

### 4.2. Absorption TRI

Absorption TRI effects are shown in Fig. 6. For the two optical thicknesses that have been

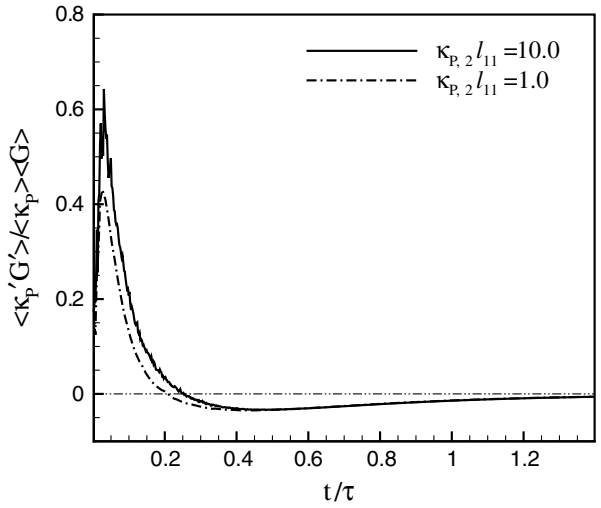


Fig. 6. Evolution of absorption coefficient—intensity correlation factor $\mathcal{R}_{\kappa G}$ with nondimensional time.

examined, $\mathcal{R}_{\kappa G}$ departs from unity and shows similar trends as the emission TRI. The periodic boundaries in the three directions yield $\langle \nabla \cdot \vec{q}_{\text{rad}} \rangle = 0$: all radiation that is emitted in the box eventually is absorbed in the box. The incident radiation $G$ then acts as an averaging operator for the radiation intensity over the domain, as $G$ is determined by radiation incident from all directions. This results in the absorption correlation factor (determined by effects from all over the domain) being lower than the emission correlation factor (determined locally). The horizontal dash-dot-dot reference line in Fig. 6 corresponds $\mathcal{R}_{\kappa G} = 0$ (absence of absorption TRI).

## 5. Conclusion

Direct numerical simulation coupled with a radiation photon Monte Carlo method has been used to explore turbulence–radiation interactions in an idealized nonpremixed system. The temperature self-correlation, absorption coefficient—Planck function correlation, and absorption coefficient—intensity correlation have been isolated and quantified to study TRI effects. At intermediate-to-large values of the optical thickness, contributions from all three correlations are significant. These results imply that ignoring TRI effects for nonpremixed turbulent reacting flows may result in significant errors. For the particular functional form of $\kappa_{\text{P}}(Y_{\text{P}}, T)$ that has been adopted here, it has been found that both $\langle \kappa'_{\text{P}} I'_b \rangle$ and $\langle \kappa'_{\text{P}} G' \rangle$ can be negative under some conditions. Favorable results for emission TRI have been obtained using a simple $\beta$ PDF model. This suggests that a relatively simple model for emission TRI may be constructed by modeling the variance of the mixture fraction in nonpremixed chemically reacting flows. Recent studies of Wu et al. [11] and Deshmukh et al. [22] have included effects of feedback and finite-rate chemistry in their TRI studies. In future work, DNS will be used to explore advanced scenarios involving complex chemistry, nongray-gas radiation and soot radiation with full coupling.

## Acknowledgment

This work has been supported by the National Science Foundation under Grant Number CTS-0121573.

## References

[1] M.F. Modest, *Radiative Heat Transfer*, second ed., Academic Press, New York, 2003.
[2] A. Townsend, *J. Fluid Mech.* 3 (1958) 361–375.
[3] T.H. Song, R. Viskanta, *J. Thermophys. Heat Transfer* 3 (1987) 52–62.
[4] A. Soufiani, P. Mignon, J. Taine, *Proc. Ninth Int. Heat Transfer Conf.* 6 (1990) 403–408.
[5] R.J. Hall, A. Vranos, *Int. J. Heat Mass Transfer* 37 (1994) 2745.
[6] S.R. Tieszen, *Ann. Rev. Fluid Mech.* 33 (2001) 67–92.
[7] S. Mazumder, M.F. Modest, *Int. J. Heat Mass Transfer* 42 (1998) 971–991.
[8] G. Li, M.F. Modest, *J. Quant. Spectrosc. Radiat. Transfer* 73 (2002) 461–472.
[9] P.J. Coelho, *Combust. Flame* 136 (2004) 481–492.
[10] L. Tessé, F. Dupoirieux, J. Taine, *Int. J. Heat Mass Transfer* 47 (2004) 555–572.
[11] Y. Wu, D.C. Haworth, M.F. Modest, B. Cuenot, *Proc. Combust. Inst.* 30 (2005) 639–696.
[12] Y. Wu, M.F. Modest, D.C. Haworth, A high-order photon Monte Carlo method for radiative transfer in direct numerical simulation of chemically reacting turbulent flows, *J. Comp. Phys.* (submitted) (2005).
[13] V.P. Kabashnikov, G.I. Kmit, *J. Appl. Spectrosc.* 31 (1979) 963–967.
[14] V.P. Kabashnikov, *J. Eng. Phys.* 49 (1985) 778–784.
[15] V.P. Kabashnikov, G.I. Myasnikov, *Heat Transfer-Soviet Res.* 17 (6) (1985) 116–125.
[16] D.C. Haworth, T.J. Poinsot, *J. Fluid Mech.* 244 (1992) 405–436.
[17] M. Baum, Etude de l'allumage et de la structure des flames turbulentes, Ph.D. thesis, Ecole Centrale de Paris (1994).
[18] V. Eswaran, S.B. Pope, *Phys. Fluids* 31 (3) (1988) 506–520.
[19] Combustion Research Facility, Sandia National Laboratories, *International Workshop on Measurement and Computation of Turbulent Nonpremixed Flames* (http://www.ca.sandia.gov/TNF/radiation.html, 2002).
[20] S. Lele, *J. Comput. Phys.* 103 (1992) 16–42.
[21] R.W. Bilger, *Turbulent flows with nonpremixed reactants, in: Turbulent Reacting Flows*, Springer, Berlin, 1980, pp. 65–113.
[22] K.V. Deshmukh, M.F. Modest, D.C. Haworth, in: *Proceedings of Eurotherm Seminar 78,* Poitiers, France, 2006.

## Comment

*Jay Gore, Purdue University, USA*. What is the effect of TRI on the heat flux absorbed at the boundary? What are the effects of length and time scales of turbulence on the heat flux and the radiation source term?

*Reply*. In this work, we have focused on isolating key statistical correlations that pertain to TRI in a highly idealized canonical configuration, rather than on global influences of TRI on mean temperature, the radiation source term, and heat fluxes. These global effects will be configuration dependent, and are being examined in ongoing work and in other configurations.

It is anticipated that the most important influence of turbulence length scales should be through the dimensionless optical thickness at the scales of the turbulence. Here the optical thickness based on the turbulence integral length scale has been varied by changing the absorption coefficient. More systematic investigations of the effects of turbulence scale effects are in progress.